EUROPEAN ORGANIZATION FOR NUCLEAR RESEARCH

CERN/PPE/92-200
5 November 1992

First observation of Cherenkov Rings in a Fast RICH Detector combining a Cesium Iodide Photoconverter with an Atmospheric Pressure Wire Chamber

F. Piuz 1), A. Braem 1), G. Paic 1,2), R.S. Ribeiro 1), T.D. Williams 1)

1) CERN, Geneva, Switzerland
2) Ruder Boskovic, Zagreb, Croatia

Abstract

A Ring Imaging Cherenkov Detector, combining a sodium fluoride radiator with a CsI photoconverter evaporated on the pad cathode of a wire chamber, has been built and tested in a particle beam. Systematic measurements of the number of photoelectrons per Cherenkov ring indicate that the quantum efficiency is 60–70% of the one measured in the same detector filled with TMAE. The preliminary results demonstrate the technological feasibility of such large area fast RICH detectors.

To be submitted to Nuclear Instruments and Methods

1. INTRODUCTION

The Ring Imaging Cherenkov (RICH) technique is a powerful tool for particle identification in high energy physics experiments. Until now, the UV photons emitted from a radiator were detected preferably using detectors containing photosensitive vapors, TMAE or TEA, which often causes delicate problems of construction and operation. The electrons created in the gaseous volume were recorded in different ways, such as TPC, pad read-out [1], avalanche light recording [2].

The advent of CsI photocathodes operating in reflective mode [3] has opened a new possibility to detect UV photons in a well defined plane, simplifying the detector design and eliminating the tedious operation with photosensitive vapors. A particularly well suited application is the use of the "proximity focusing" geometry [4] where the Cherenkov photons, issued from a thin solid or liquid radiator, are detected in a wire chamber. In this case, the photon conversion and the photoelectron detection can be performed by a two dimensional array consisting of the pad cathode of the wire chamber. The resulting "fast RICH detector", allows for recording events of very high multiplicity, $\geq 50/m^2$, since the sensitive detection volume for particles and photoelectrons can be made very thin. Such requirements are found in an experiment proposed at the CERN Large Hadron Collider operated with heavy ion [5] or in HADES, another heavy ion experiment planned at GSI [6].

We report here on the first tests of a fast RICH detector, combining a solid radiator with a pad cathode covered with a thin layer of CsI photoconverter.

2. APPARATUS AND ELECTRONICS

A fast RICH detector, of the type shown in fig. 1, was previously used to study Cherenkov rings with TMAE as a photosensitive medium. Experimental results, obtained with solid NaF and liquid Freon radiators are discussed in refs. 7,8.

TMAE vapours were enclosed in the detection volume, namely the MWPC formed by the transparent cathode, the sense wire plane and the pad cathode as shown in fig.1. A quartz plate (not shown) was implemented against the transparent cathode, enabling the Cherenkov photons to propagate in a UV transparent gas (N_2) filling the gap between the radiator and this plate.

The detector layout has been modified when replacing TMAE by a thin solid CsI photosensitive layer evaporated on the pad cathode. This layer acts as the sole photosensitive agent, as proposed in [3]. In this case, the quartz plate is suppressed and the entire detector volume is filled with a UV-transparent gas mixture (methane/isobutane 97/3).

An additional wire electrode is implemented close to the radiator. It is held at a small positive potential with respect to the grounded transparent cathode in order to collect the primary ionization deposited by the charged particles between the two electrodes, hindering an unnecessary amplification in the photon detector.

The photon detector is a wire chamber (MWPC), having a 2 mm distance between the transparent cathode and the anode wires plane. The distance between the anode wires and pad cathode plane was adjustable between 1 mm and 2 mm for test purposes. It was essentially kept at 2 mm. The transparent cathode is made either of 50 μm diameter stainless steel mesh with a 500 μm pitch or 100 μm diameter wires with a 2 mm pitch. The pitch of the anode wires is 4 mm, their diameter is 20 μm. The size of the cathode pads is 8×8 mm^2. The sense wires are positively biased while the cathodes are

grounded.The signals induced at the pads are read out by means of an analog multiplexed electronic chain. The front end element is a 16 channels VLSI chip, AMPLEX, [9]. A peaking time of 400 nsec is used and the threshold corresponds to an equivalent charge reported at the input of 0.6 fC.

The signals from the sense wires are also read out.

3. PREPARATION OF THE SOLID PHOTOCATHODE

For these first measurements, the preparation of the CsI pad photocathode was performed in the simplest way:

- the pad electrode is made by an usual printed board technology, namely copper etching on G-10 epoxy resin substrate, followed by chemical gold plating. No further layer was deposited on this electrode. The total pad area is 300×120 mm^2.
- the electrode was installed in the evaporating vessel with its back side, where electronics connections are implemented, protected by a tight box allowing for a primary vacuum to be achieved. This avoids long outgassing and pollution of the high vacuum necessary for CsI evaporation. It was possible to heat the electrode for outgassing up to 70 °C.
- a continuous CsI layer was evaporated, covering the metallized pads as well as the separation gaps between them (G-10). The distance source-to-electrode was 36 cm, the evaporation rate was 4 to 10 nm/sec and the pressure during evaporation was 5 to $15 \cdot 10^{-7}$ Torr. At the beginning of the evaporation, the source was screened by a shutter.
- a mask was installed at a corner of the sensitive area letting several pads uncoated with CsI, to allow for single electron measurements with the UV light to be compared with similar measurements on coated pads.
- after the coating process, the evaporation chamber was vented (nitrogen or methane) and the pad cathode was immediatly mounted on the UV detector. That operation implied an exposure to air for about 20 minutes. The detector was then flushed with argon, closed, and mounted at the experiment. It was then flushed at about 20 l/hour with the operating gas, namely a mixture of methane/isobutane 97/3 in volume, at atmospheric pressure for the rest of the experiment.

4. EXPERIMENTAL SETUP AND PROCEDURES

The detector was installed at the PS/T11 beam line at CERN. A mixed beam of pions and protons of 3 GeV/c was chosen (β pion = 0.9989, β proton = 0.9544).

A Time of Flight facility provided the possibility of an on line particle selection .

The distance between the radiator (10 mm thick NaF) and the pad cathode was adjusted such as to achieve a 39 mm Cherenkov ring radius for protons (refractive index = 1.39), suited to our sensitive area of 12×12 pads. The pion ring diameter exceeds this area.

The event trigger was given by the time coincidence of 4 small scintillators defining a beam spot at the chamber of about 5×5 mm^2. However, the beam size being much larger than this spot, the whole chamber was submitted to a particle flux of about 1-3 kHz per sense wire.

Recent evaluations [10,11] of the quantum efficiency of CsI photocathode emphasized the virtue of heating the photocathode (> 45°C) under a flow of methane in order to enhance the quantum efficiency. The whole detector was then enclosed in a box allowing it to be heated up to 70°C. The gases in use were of 99.95 purity. The distribution system was equipped with purification devices (Oxy- and Hydrosorb), oxygen control and water vapor admixture capability.

The Pulse Height (PH) distribution of single electrons was monitored, being an essential tool for the evaluation of the quantum efficiency of the photocathode. For this purpose, two quartz windows allowed to illuminate the pad cathode with a UV light beam (Deuterium lamp) and extract single electrons by photoelectric effect. That could be done on pads coated and not coated with CsI.

Such measurements were taken before or/and after each run with beam particles.

5. BASIC MEASUREMENTS WITH THE DETECTOR

5.1 Detection of charged particles

By positively polarizing the collection mesh (100V), mostly the primary ionization deposited by the charged particles inside the thin MWPC is amplified at the sense wires. Therefore the localization accuracy, obtained by centroid calculation (about 0.5 mm), is preserved independently of the incident angle of the particle trajectory.

Figure 2 shows the mean number of pads hit per particle at normal incidence as a function of the high voltage. A mesh cathode restricts almost completely the collection of primaries to those deposited within the MWPC gap. A wired cathode of 2 mm pitch was also tested owing to its superior transparency to the Cherenkov light. Only a small increase of the number of pads hit per particle was observed in this case since the collection time of the primaries is larger than the integrating time of the pad electronics.

In fact, the drift field established in the proximity gap sets the electron drift velocity at a low value, about 10 mm/μsec in pure methane [12]. Since the chamber gain is raised so as to efficiently detect single electrons in the case of Cherenkov ring imaging, the detector operates in a "cluster counting" mode, remembering [13] that the primary ionization is composed of a large fraction of well separated single electrons. Therefore, the electrical transparency should be kept at a minimum level in order to avoid late collection of charges, being possibly mixed to a different event.

Measurements performed with CsI-coated and uncoated pad electrodes show no influence of the coating on the operation of the wire chamber. Gain and stability were found identical under particle flux up to 3 kHz per wire.

5.2 Detection of Single Electrons

The previous remark applies as well to the measurements performed with single electrons. Using the same UV flux, an optical attenuation of 200 was necessary in order to achieve the same counting rate at the sense wire (3-5 kHz) when the pads coated with CsI were illuminated.

Figure 3 shows the expected exponential PH distribution measured at the pads. Let us denominate A_0 the slope evaluated within the straight (purely exponential) part of such a distribution. The "cut" at the left part of the spectrum originates from the threshold applied to the wire electronics used to trigger the pad readout in this particular

measurement. The pad threshold values, A_{th}, are typically 3-4 ADC units, expressed in the same unit as in fig. 3.

The detection efficiency of single electrons can be evaluated as $\varepsilon_{sing} = \exp(-A_{th}/A_0)$. However, due to the discrete pad structure, this value depends significantly upon the position of the avalanche along the wire with respect to the pad array [7].

Figure 4 summarizes the results of different measurements as a function of anode voltage, recorded at the pads and at the sense wires (also shown for comparison, the charged particle results). A detection efficiency of 75% is found at 2100 V. Knowing the fraction of the total charge measured at the respective integrating times of the wire (20% at 50 nsec) and pad electronics (40% at 400 nsec), the gain of the chamber is found to be about $1.0 \cdot 10^5$ at 2000 V.

6. CHERENKOV RINGS

We present below the results obtained with several photocathodes, differently processed and submitted to various sequences of treatments after being mounted on the detector. The main results are summarized in table 1.

6.1 Evaluation of the Quantum Efficienty of the solid Photocathode using Cherenkov Rings and Pad Read Out

The number of Cherenkov photons, N_{ch}, emitted from a radiator of length L_o with a refractive index n at an angle $\theta = \cos^{-1}(1/\beta n)$, converted, after having travelled through the detector, into an equal number N_{pe} of photoelectrons at the CsI photocathode of quantum efficiency ε_{qe}, is given by:

$$N_{pe} = N_o \cdot L_o \cdot \sin^2\theta$$

with

$$N_o = 370 \int_{(\Delta E)} \varepsilon_1 \varepsilon_2 \varepsilon_3 \varepsilon_{grid} \varepsilon_{qe} \, dE$$

We describe below the procedures used to evaluate N_o, N_{pe}, ΔE. Once these quantities known, the value of the quantum efficiency $\varepsilon_{qe}(E)$ integrated over the spectral photon range ΔE is obtained.

i) The quality factor, N_o.

It takes into account all photon losses and implies five terms which are respectively the integrals over the spectral range ΔE of the optical transparency of the NaF radiator, the optical reflexion at the NaF interface, the optical transparency of the gas mixture, the optical transparency of the cathode at the incident angles in question and the quantum efficiency of the CsI photocathode. Since the measurements were taken with particles of $\beta = 0.9544$, it has been shown in [7] that the loss by total reflexion in the NaF radiator can be neglected.

To calculate the quantum efficiency, we took the following values, measured or calculated for the geometry and the particle energy in use:

$$\varepsilon_{grid} = 0.62 \text{ (mesh)}, 0.88 \text{ (wires)}, \varepsilon_1 = 0.85, \varepsilon_2 = 0.92, \varepsilon_3 = 0.95$$

ii) The spectral photon range, ΔE.

The measurements of the number of pads hit per ring were taken in a sensitive area of 12×12 pads, limiting the maximum size of a full ring radius to 46 mm. That radius corresponds to a value of the NaF refractive index of 1.41 taking into account the

distance radiator/pad cathode in use (see sect. 4) and the NaF chromaticity [4]. That is in fact equivalent to apply an upper cut to the Cherenkov photon spectrum at about 175 nm (7.1 eV). The low energy limit is determined by the photoionization threshold of CsI taken at 220 nm (5.6 eV) [3,11].

iii) The number of initial photo electrons, N_{pe}

We have to deduce N_{pe} from the measured mean number of pads hit per ring, N_{pad}, that is to take into account the detection efficiency of single electrons in our various operating conditions.

To use only the quantity ε_{sing} as defined in sect. 5-2 is not sufficient since:

- the sharing of the induction makes the detection efficiency dependent of the position of the avalanche along the wire,
- PH overlaps are possible due to the number of photo electrons in the ring
- the threshold values are pad dependent.

Therefore, we used a programme simulating the response of the pad detector to single electrons by generating photons through the experimental layout in a chosen ΔE range. For a fixed N_{pe}, PH pad patterns associated to a ring are generated by overlapping the PH contributions obtained by drawing:

- for every electron, a PH value in an exponential distribution of slope A_0. Knowing the position and the shape of the induction spread [7], the corresponding PH pattern is generated,
- for every pad, a noise contribution in a measured pedestal distribution.

Then, a threshold is applied at every pad. It is defined as:

$$TH_i = PED_i + N \, . \, SIG_i$$

where SIG_i is the standard deviation of the pedestal distribution of mean PED_i at every channel i, N being an adjustable non integer constant.

Repeating this procedure a fixed geometry and particle energy for different choices of (N_{pe}, A_0, N), one obtains the dependence between the expected number of pads hit and the number of initial photo electrons N_{pe} per ring, defined as:

$$N_{pad} = K \, N_{pe}$$

where K is a function of N_{pad}, A_0, N. An exemple of calculation is shown in fig. 5.

iv) Data taking and analysis.

We had two modes for reading out the pads:

- a "zero suppression" or "online" mode, where data are compared to pedestal/threshold tables stored in the readout card. That implies a fixed value of N and integer values of PED_i and TH_i. In that case hit pads are retained if enclosed in a fiducial zone of 12×12 pads excluding the central 4×4 pads region where the charged particle clusters occur.
- a "full" read out or "offline" mode, where all pads are read out by setting PED_i and TH_i values to zero. Pedestals distributions have to be recorded as well. A minimum, non integer value, of N can be found by offline analysis as the value at which a change of slope occurs in the plot of the number of pads above threshold

versus N. In that case, the fiducial zone is enclosed between two circles of radii defined according to point ii) of this section, also taking into account the radiator chromaticity, the spread due to the radiator thickness and the finite extension of the triggering area.

- In table 1, we present results obtained with both modes. The integral of the quantum efficiency is only calculated in the offline case where the spectral range ΔE is well defined. The online results can be compared between themselves. Their mainly higher values reflects the larger ΔE associated to the squared fiducial zone used.

6.2 MEASUREMENTS OF CHERENKOV RINGS

In the present beam test four photocathodes were used. Their specification in production and testing procedures are described below.

i) The first photocathode 0.5 μm thick, was evaporated at a vacuum of about 3. 10^{-6} Torr.

During ten days, the measurements were taken in the following sequence:

a. at ambient temperature
b. at 42 °C, after 12 hours heating
c. at ambient temperature, after 12 hours heating at 65°C

the detector being kept under a constant gas flow of 20 l/hour without any purification devices.

ii) Before evaporating the second photocathode (0.5 μm thick), the pad substrate was outgassed at 60°C under vacuum for 12 hours. The evaporation was performed at 5×10^{-7} Torr. Then, the vessel was filled with methane at 100 Torr for 1 hour.

During ten days, the measurements were taken at ambient temperature under a constant 20 l/hour gas flow in the following sequence:

a. no purification devices
b. with Oxy- and Hydrosorb filters
c. after one hour flushing with dry air
d. after bubbling the gas mixture through water at 2 °C for 1 hour, (equivalent to about 6000 ppm water)
e. after heating the detector at 50°C for 24 hours

iii) The third photocathode was processed as in ii), except that the CsI layer thickness was 1.8 μm. The measurements were taken as in ii)-b during 24 hours.

iv) The fourth photocathode was processed as in ii) except that the substrate was kept at 60°C during the evaporation. The measurements were taken as in ii)-b:

a. during 24 hours after mounting the photocathode
b. during 24 hours after ten days of flushing with the gas mixture
c. during two days, with pure methane, after 3 days of flushing.

The "mesh" transparent cathode ($\varepsilon_{grid} = 0.62$) was used only during the test of the first photocathode. Due to the field distorsion introduced by the "wired" cathode ($\varepsilon_{grid} = 0.88$), the voltage had to be raised by 50 V to reach about the same gain.

Figure 6 shows an exemple of a single event pad pattern.

In figure 7, we present some of the distributions obtained during a run and following the offline analysis described in section 6-1. In this analysis, the ring radius is calculated as the average of the distance between the particle impact and the centres of every pad belonging to the ring. For the moment, the impact point determination is very coarse within the triggering area of 5×5 mm^2.

7. DISCUSSION

After the various CsI layer processings and their treatments in the detector, we can make the following observations about the quantum efficiency of the photocathode:

- Exposing the layer to dry air flow or to water vapor has little influence and, if any, the initial value can be recovered. It seems that the first exposure to air when the photocathode is mounted on the detector determines the state of the surface and its properties.
- Heating the photocathode under methane flow has the effect of lowering the quantum efficiency (by 20%). It might be possible that the initial value could be recuperated after a longer time . In fact, we observed a slight improvement over a period of time of two days. However, we do not observe the spectacular increase by a factor of $\approx$2 following this treatment as reported by Anderson [11].
- Since our G-10 substrate is very coarse, we tried a thicker layer hoping for a superior coverage of the deposit. Indeed, we observed several high voltage trips at the first rising of the voltage up to the working value, 2050 V, possible indication of a better continuity of the layer, therefore of a superior insulation. However, the initial value of ε_{qe} was lower, slowly improving with time.
- Heating the substrate during the evaporation might influence the nucleation of the layer. The initial measurement of the quantum efficiency was found slightly lower than before but improved by 20% after a long period of flushing. Operating the chamber with pure methane still gave a 15% increase. For the moment, it is not possible to attribute this further improvement to the use of pure methane: it might as well be the same trend to improve with time observed all along these tests or a photon feedback effect due to the lack of isobutane.

Considering the results measured after two days and more of operation at ambient temperature, we have ten measurements of the CsI quantum efficiency integrated over 1.5 eV ranging between 0.166 and 0.213. The systematic error on the integrated quantum efficiency,attributed to the K determination, is estimated to be $\pm$ 10%.

Approximating the ε_{qe} dependence versus the photon energy to be linear within ΔE, we find a value of 22–28% at 175 nm for the quantum efficiency of the CsI photocathodes.

One should notice that it is the first measurement of the CsI quantum efficiency using an intrinsic single UV photon source, namely the Cherenkov effect. Another fact to remark is that the measurement was performed under gas multiplication, implying a high flux of positive charges bombarding the photocathode.

This result can be compared to results obtained by the measurement of the photoelectric current emitted from a calibrated high flux of monochromatic UV photons or pulsed photon source in amplification mode. In both cases, the photon flux calibration is cross-checked by measuring the known quantum efficiency of TMAE. From these methods, the best results quoted for quantum efficiencies integrated over the range 175-

220 nm are 0.26 by Seguinot et al [3] and 0.08 by Brauning et al [10] under methane flow at atmospheric pressure. An integrated value of 0.30 is found by Anderson et al [11] in pulsed mode under methane at 20 Torr. Using wire chamber technique, Arnold et al quoted in [14] values of 16% and 7% at respectively 160 and 200 nm; the best result reported by Cindro et al [15] is about 80% of the Seguinot et al's measurement at 170 nm.

It should be noted that the quantum efficiency measured here is compatible with our results reported for the same chamber in the same setup but using hot TMAE vapors as photo converter [7,8].

Following a discussion found in [8], the ring radius accuracy presently measured would allow to achieve a 3 sigma separation between pions and kaons up to 2 GeV/c, using rings of 100 mm radius at $\beta = 1$, as shown in fig 8.

It is important to note that the results presented here are already significant for particle identification intended in the range of 0.7 to 2 GeV/c [5] and other applications [6].

8. CONCLUSIONS

A first test of four Cesium Iodide photocathodes deposited as a continuous layer on a 30×12 cm^2 pad electrode has been performed in a fast RICH structure. A wire chamber, operated under methane/isobutane flow at atmospheric pressure and ambiant temperature, was used as a photo electron and charged particles detector.

The detector has shown very stable operation at a gain allowing for a single electron detection efficiency of 75%.

The CsI quantum efficiency integrated over a photon energy range of 1.5 eV, obtained from 10 measurements of four photocathodes, ranged between 0.166 and 0.213, corresponding to values of 22-28% of the quantum efficiency at 175 nm.

Under the limit of detection sensitivity settled by our present electronics, Cherenkov rings were recorded with up to 9–10 photo electrons per ring. It is our intention to increase this number by developping a more sensitive electronics, preserving the present geometry and operation conditions of the wire chamber. In fact, the simple and rugged construction of the detector, allowing for an easy implementation of the pad photocathode, is a key issue for the realization of large area and cost effective UV-photon detectors.

Noticing that the transfer of the fresh photocathode from the evaporation vessel to the detector was performed under air, further controlled exposures to dry air or water vapor have been found of little influence on the quantum efficiency of the photocathodes.

However, we have not observed any quantum efficiency enhancement after the heating of the photocathode up to 65°C under Methane flow, as reported from other authors' work [11].

9. ACKNOWLEDGMENTS

The authors would like to acknowledge Mr D. Carminati from CERN, taking charge of the CsI evaporation and thank our colleagues of the CERN Research and Development Project RD26, A. Breskin from the Weizmann Institute and E. Nappi from the Bari University for their efficient contributions.

One of us (G.P) would like to thank CERN, INFN-Bari and the University of Giessen for support.

REFERENCES

[1] R. Arnold et al, Nucl. Instr. and Methods, A252 (1986) 188.

[2] J. Baechler et al, CERN/PPE/92-111.

[3] J. Seguinot et al, Nucl. Instr. and Methods A297 (1990) 133.

[4] R. Arnold et al, Nucl. Instr. and Methods A273 (1988) 466.

[5] Heavy Ion Experiment at LHC, J. Schukraft, Towards the LHC Experimental Programme, March 1992, Evian-les-Bains.

[6] HADES experiment, letter of intent in preparation, GSI, Darmstadt.

[7] F. Piuz et al, pg 121-142, 4th San Miniato Topical Seminar, Experimental Apparatus for High Energy Physics and Astronomy, eds P. Giusti et al, 1990, World Scientific.

[8] F. Piuz et al, presented at the 3th International Conference on Advanced Technology and Particle Physics, Villa Olmo, June 1992, submitted to Nucl. Instr. and Methods.

[9] E. de Beuville et al, Nucl. Instr. and Methods A288 (1990) 157

[10] H. Brauning et al, WIS-92/62/Aug-PH, The Weizmann Institute, Rehovot, submitted to Nucl. Instr. and Methods.

[11] D. Anderson et al, presented at the 3th International Conference on Advanced Technology and Particle Physics, Villa Olmo, June 1992, submitted to Nucl. Instr. and Methods.
D. Anderson et al, FERMILAB Pub 92/285, October 1992, submitted as a Letter to the Editor in Nucl. Instr. and Methods.

[12] F. Piuz, Nucl. Instrm. Methods 205 (1983) 425.

[13] F. Lapique et al, Nucl. Instrm. Methods 175 (1980) 297.

[14] R. Arnold et al, CRN/HE 91-06, Centre de Recherches Nucleaires, Strasbourg.

[15] V. Cindro et al, presented at the 3th International Conference on Advanced Technology and Particle Physics, Villa Olmo, June 1992, submitted to Nucl. Instr. and Methods.

Table 1- The first column refers to the various photocathodes and their tests as described in sect. 6-2. The thresholds were calculated with N=4 or 5(*) for online results, and with N = 3 for offline results. The first photocathode (i) was tested with a grid where $\varepsilon_{grid} = 0.62$. A_0 is the mean PH for single electrons. The barometric and temperature variations are partly responsible of the A_0 fluctuations.

photocathode/ process	H.V kV	#	pads/ring online	A_0 ADC ch	K	# pads/ring offline	$\int \varepsilon_{qe}\, dE$
i-a	1.95	*	4.5 ± 2.5	3.5			
	2.00	*	6.5 ± 3.2	5.6			
	2.05	*	8.3 ± 4.0	8.9			
i-b	2.00	*	5.3 ± 3.0				
	2.05	*	7.5 ± 3.9				
i-c	2.05	*	5.3 ± 3.3				
	2.05		6.0 ± 3.7	7.4			
	2.10		8.4 ± 4.4	12.0			
ii-a	2.00	*	5.7 ± 3.8				
	2.05	*	8.5 ± 4.0				
	2.10	*	11.1 ± 4.4				
	2.05		10.8 ± 4.3	6.9	0.58	10.4 ± 4.2	0.171
	2.10		14.8 ± 5.3	10.4			
ii-b	2.05		13.5 ± 4.9	7.4	0.62	11.1 ± 4.2	0.171
ii-c	2.05		10.5 ± 4.2	6.8	0.58	10.3 ± 4.2	0.170
ii-d	2.05		8.0 ± 3.8				
	2.05		10.8 ± 4.1	7.2	0.60	9.8 ± 4.2	0.156
ii-e	2.05		8.4 ± 3.8	7.4			
iii-a	2.05		8.4 ± 4.0	7.0			
iv-a	2.05		8.7 ± 4.2				
	2.05		9.8 ± 4.6	7.4	0.62	8.8 ± 4.4	0.136
	2.10		12.2 ± 4.2	12.0	0.85	12.9 ± 5.6	0.145
	2.00		7.1 ± 3.8	5.2	0.46	6.8 ± 3.6	0.138
iv-b	2.05		11.2 ± 4.1	8.7	0.70	12.3 ± 4.5	0.168
	2.00		7.3 ± 3.4	5.1	0.46	8.5 ± 3.5	0.176
	2.10		14.2 ± 4.8	12	0.85	14.8 ± 5.1	0.166
iv-c	2.05		13.6 ± 4.4	8.2	0.65	12.2 ± 4.6	0.180
	2.05		12.6 ± 4.4	6.5	0.56	12.5 ± 4.8	0.213
	2.10		16.6 ± 5.8	9.8			
	2.10			10.8	0.78	15.1 ± 5.2	0.185
	2.00		8.2 ± 3.7	5.3	0.47	8.1 ± 3.8	0.172

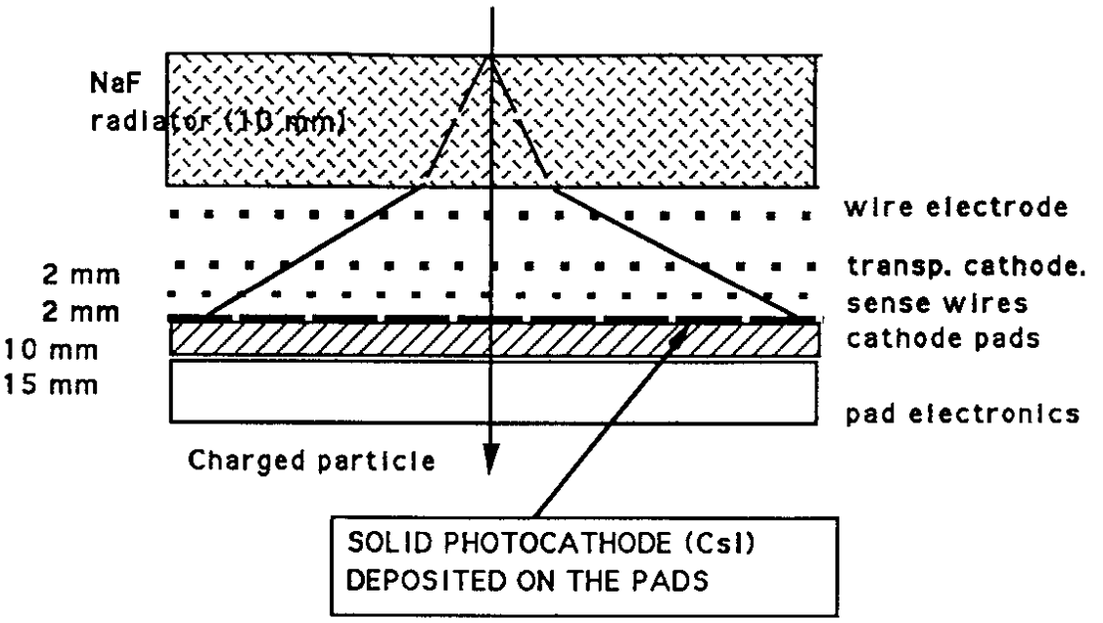

Figure1: Schematic drawing of the fast RICH with a solid photocathode

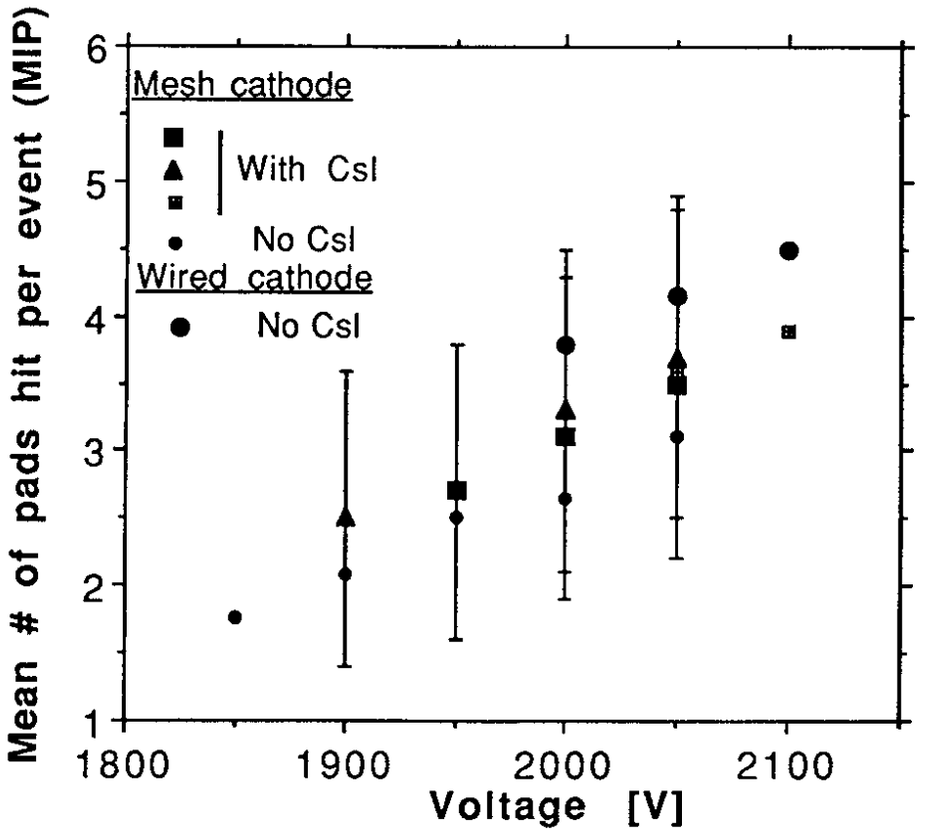

Figure 2: Mean number of pads hit per particle at normal incidence using coated and uncoated pad cathodes. Two different transparent cathodes are used.

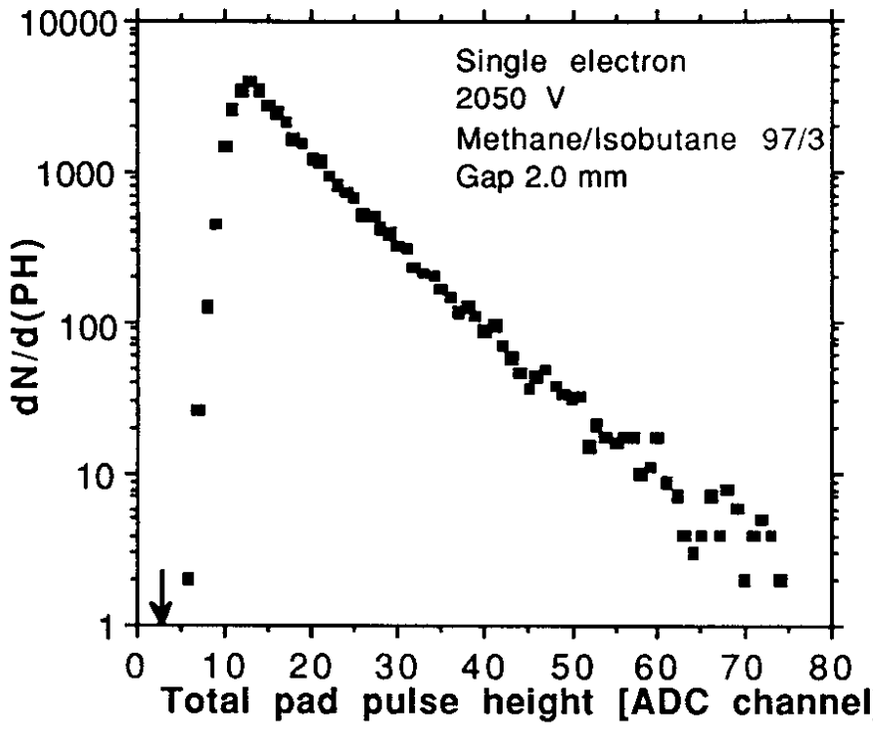

Figure 3: Pulse height distribution for single electrons obtained with a UV lamp measured at the pads. The arrow indicates the typical value of the pad electronics threshold. In this measurement, the threshold value is imposed by the wire electronics.

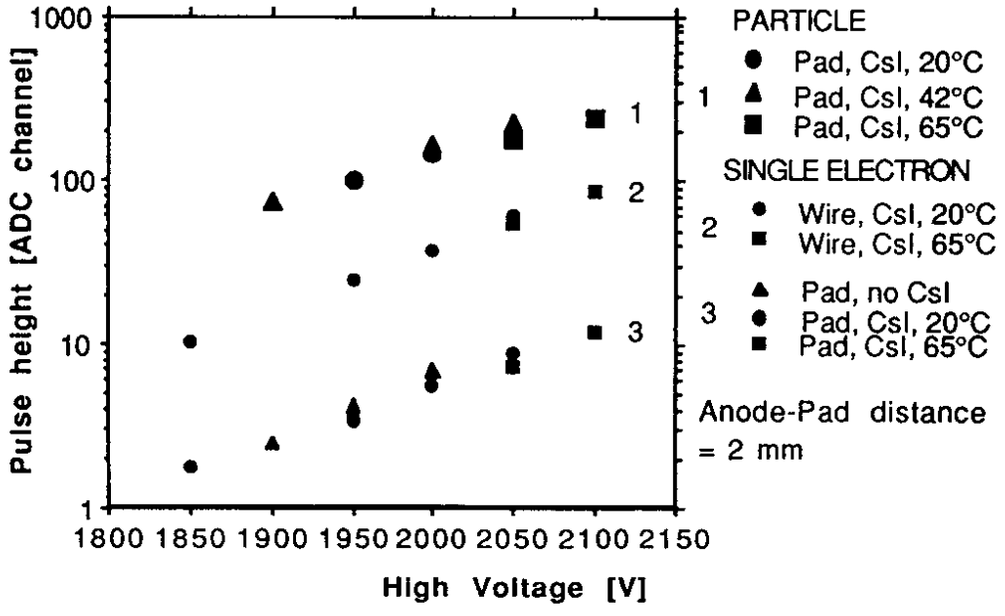

Figure 4: Mean pulse height values in function of the anode voltage measured at the wire or at the pads. They are obtained from single electrons and particles.

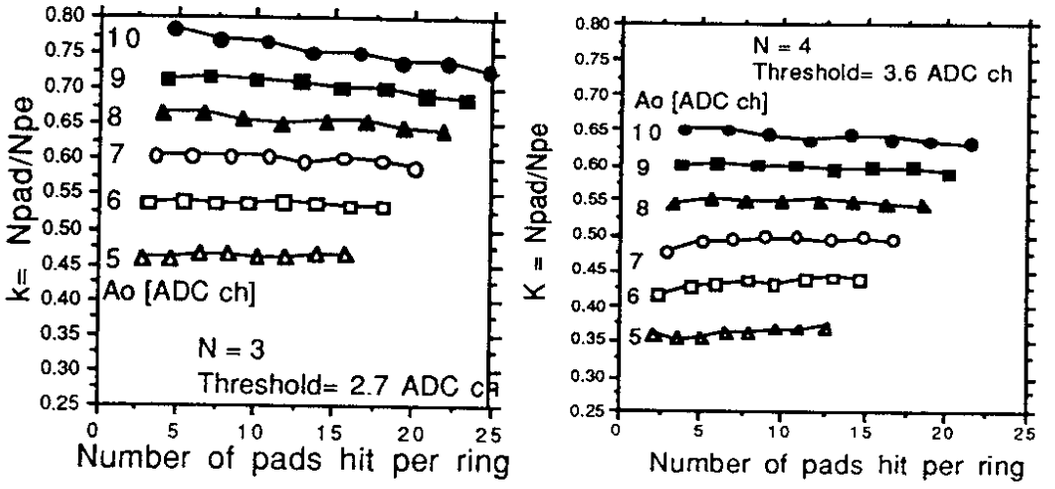

Figure 5: Results of the simulation calculating the number of pads hit, above threshold, for initial photoelectrons distributed around a ring of mean radius 39 mm. The conditions are: 3 GeV/c protons, NaF radiator 10 mm thick, ΔE=1.5 eV, MWPC geometry as described in sect. 2. Ao is the mean PH for single electrons.

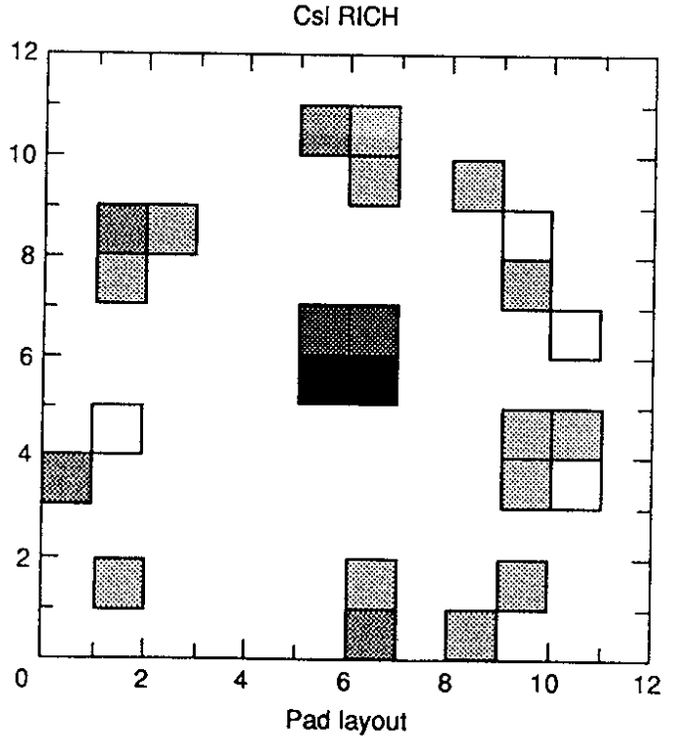

Figure 6: Pad read out display of a typical Cherenkov event. The central particle and single photo electrons are visible. The shades represent the different charges collected.

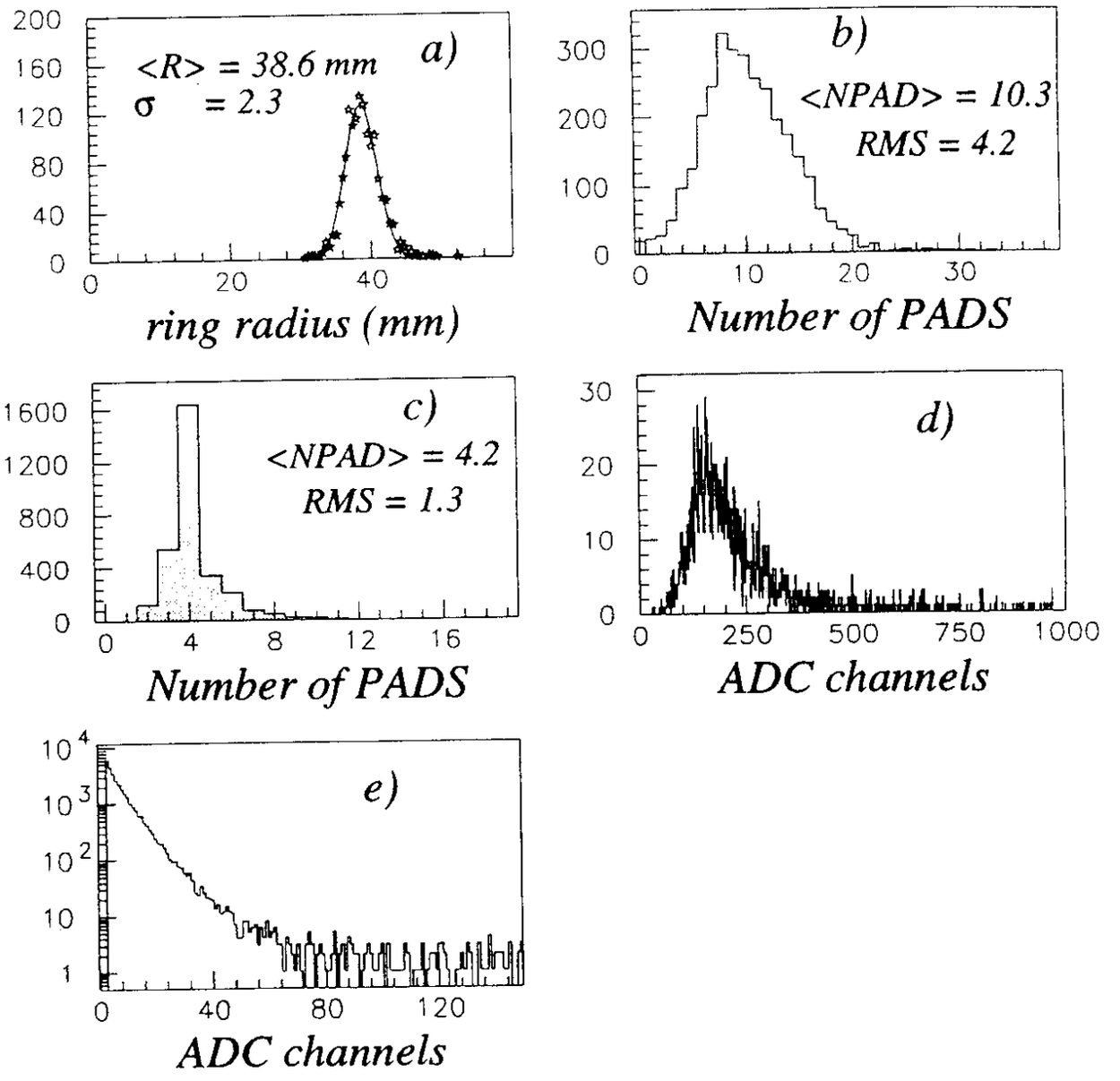

Figure 7: Distributions of the radii (a), number of pads hit per ring (b) and in the central part where the particle hits the detector (c). (d) shows the "Landau shaped" total pad PH distribution per particle measured in the central region. (e) is the "exponential shaped" single pad PH distribution measured in the ring region.

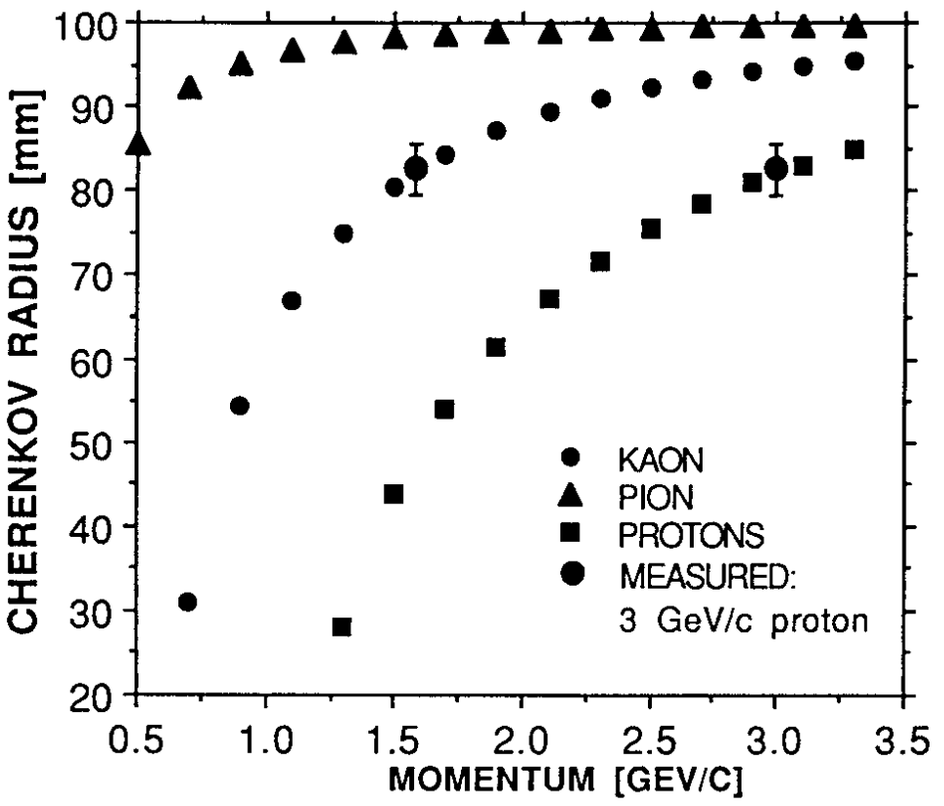

Figure 8: Calculated dependence of the ring radii on incident momenta for pions, kaons and protons with the spread measured in this work. The point on the kaon line is derived from the proton one since only the β value of the particles counts.